(This is a sample cover image for this issue. The actual cover is not yet available at this time.)

Stem Cell Research (2014) 12, 815–827

Available online at www.sciencedirect.com

ScienceDirect

www.elsevier.com/locate/scr

ATF3 is a novel nuclear marker for migrating ependymal stem cells in the rat spinal cord

Miranda Mladinic[a,b,c,*], Elena Bianchetti[a], Ana Dekanic[a,c], Graciela L. Mazzone[a], Andrea Nistri[a,b]

[a] Neuroscience Dept., International School for Advanced Studies (SISSA), Trieste, Italy
[b] SPINAL (Spinal Person Injury Neurorehabilitation Applied Laboratory), Istituto di Medicina Fisica e Riabilitazione, Udine, Italy
[c] Department of Biotechnology, University of Rijeka, Rijeka, Croatia

Received 6 November 2013; received in revised form 19 March 2014; accepted 21 March 2014
Available online 30 March 2014

Abstract The present study identified ATF3 as a novel dynamic marker for ependymal stem/progenitor cells (nestin, vimentin and SOX2 positive) around the central canal of the neonatal or adult rat spinal cord. While quiescent ependymal cells showed cytoplasmic ATF3 expression, during 6–24 h in vitro these cells mobilized and acquired intense nuclear ATF3 staining. Their migratory pattern followed a centrifugal pathway toward the dorsal and ventral funiculi, reminiscent of the rostral migratory stream of the brain subventricular stem cells. Thus, the chain cell formation was, by analogy, termed funicular migratory stream (FMS). The FMS process preceded the strong proliferation of ependymal cells occurring only after 24 h in vitro. Pharmacological inhibition of MAPK-p38 and JNK/c-Jun (upstream effectors of ATF3 activation) prevented the FMS mobilization of ATF3 nuclear-positive cells. Excitotoxicity or ischemia-like conditions, reported to evoke neuronal and glial injury, did not further enhance migration of ependymal cells at 24 h, suggesting that, at this early stage of damage, the FMS phenomenon had peaked and that more extensive repair processes are delayed beyond this time point. ATF3 is, therefore, useful to identify activation and migration of endogenous stem cells of the rat spinal cord in vitro.

Introduction

The ependymal region of the adult spinal cord in mammals harbors a pool of stem and progenitor cells (SPCs) readily activated and recruited by spinal damage (Weiss et al., 1996; Hugnot and Franzen, 2011). Even though their adult neurogenesis has not been observed (Sabourin et al., 2009; Hugnot and Franzen, 2011), the neural stem cells present in the adult spinal cord are recruited and proliferate after spinal cord injury (Yamamoto et al., 2001b), producing scar-forming astrocytes and myelinating oligodendrocytes (Meletis et al., 2008). The manipulation of endogenous spinal stem cells after injury could represent one valid alternative to stem cell

Abbreviations: ATF3, activating transcription factor; AU, arbitrary units; bHLH, basic helix-loop-helix; bZIP, Basic Leucine Zipper; CC, central canal; CREB, cAMP responsive element-binding; CSF, cerebrospinal fluid; DAPI, 4,6-diamidino-2-phenylindole; DCX, doublecourtin; EdU, 5-ethynyl-20-deoxyuridine; FMS, funicular migratory stream; GFAP, glial fibrillary acidic protein; MAPK, mitogen-activated protein kinases; PM, pathological medium; RMS, rostral migratory stream; SPCs, stem and progenitor cells; TBP, TATA binding protein.

* Corresponding author at: Department of Biotechnology, University of Rijeka, Radmile Matejčić 2, 51000 Rijeka, Croatia. Fax: +385 51 584599.
E-mail address: mirandamp@uniri.hr (M. Mladinic).

http://dx.doi.org/10.1016/j.scr.2014.03.006

transplantation, since it is noninvasive and avoids the need for immune suppression (Meletis et al., 2008). Spinal stem cells are difficult to identify due to their heterogeneity and lack of specific expressional markers, since the ones currently used significantly overlap with those of mature astrocytes (McDonough and Martínez-Cerdeño, 2012). Furthermore, there is no specific marker to discriminate between quiescent and activated ependymal spinal cells, or to monitor migratory ependymal cells. Moreover, the signaling pathways and genes controlling the spinal SPC fate in normal and pathological conditions, remain largely unknown (Hugnot and Franzen, 2011). Brain transcription factors that regulate formation and proliferation of neural SPCs depend on the Sox family of genes, in particular Sox2 (Liu et al., 2013). Genomic and proteomic technologies have recently identified Wnt/beta-catenin, Notch, sonic hedgehog and growth factor networks as major signaling pathways involved in maintenance, self-renewal, proliferation and neurogenesis of the neural SPCs, and have demonstrated cross-talk between key molecules of these pathways and their modulations by transcription factors, miRNA and histone modifications (Yun et al., 2010).

At variance with the wealth of brain data, transcription factors controlling spinal cord stem cells remain incompletely understood as they have been studied with in vitro primary cultures, showing common expression of various homeodomain-type (Pax6, Pax7, Nkx2.2, and Prox1) and basic helix-loop-helix (bHLH)-type (Ngn2, Mash1, NeuroD1, and Olig2) regulatory factors in adult and embryonic rat spinal neural progenitors (Yamamoto et al., 2001a,b). In the course of our studies with biomarkers of neuronal damage (Kuzhandaivel et al., 2011) we serendipitously discovered intense immunostaining of ependymal cells for the Activating transcription factor 3 (ATF3): this observation led us to explore its expression in control or damage-induced protocols.

ATF3 belongs to the mammalian ATF/cAMP responsive element-binding (CREB) protein family of the Basic Leucine Zipper (bZIP) transcription factors (Hashimoto et al., 2002) that generate a wide range of either repressors or activators of transcription (Thompson et al., 2009). ATF3 is thought to be an immediate early gene, a stress inducible gene and an adaptive response gene, which, when activated by various stimuli, can control cell cycle and cell death machinery (Hunt et al., 2012). ATF3 promotes proliferation, motility and invasiveness of certain cancer cell lines (Wang et al., 2008; Thompson et al., 2009). ATF3 expression is normally very low in central neurons and glia, but it is markedly upregulated in response to injury and closely linked to survival and regeneration of peripheral axons (Hunt et al., 2012). Both cytoplasmic and nuclear ATF3 immunostaining has been reported with variations related to cell type, species, and injury state when it becomes prevalently nuclear (Hunt et al., 2012). ATF3 is supposed to have a role in neurite growth and regeneration (Moore and Goldberg, 2011) and it has been identified as a regulator of neuronal survival against excitotoxic and ischemic brain damage (Zhang et al., 2011). ATF3 knockout exacerbates inflammation and brain injury after transient focal cerebral ischemia (Wang et al., 2012). ATF3 has no known role in neuronal development of the intact nervous system, neither has its expression been reported in SPCs. The present study is the first report of ATF3 as a reliable marker of activated neuroprogenitor cells in the rat spinal cord.

Material and methods

Animals

The experiments were performed on neonatal or adult Wistar rats in accordance with the guidelines of the National Institutes of Health and the Italian act D.Lgs. 27/1/92 no. 116 (implementing the European Community directives no. 86/609 and 93/88), and with approval by the SISSA ethical committee for animal experimentation. All efforts were aimed at reducing the number of animals used and at minimizing their suffering. Spinal cords were dissected out from neonatal animals under urethane anesthesia (0.2 ml i.p. of a 10% w/v solution) with continuous superfusion with Kreb's solution containing (in mM): NaCl, 113; KCl, 4.5; $MgCl_27H_2O$, 1; $CaCl_2$, 2; NaH_2PO_4, 1; $NaHCO_3$, 25; glucose, 11; gassed with 95% O_2/5% CO_2, pH 7.4 at room temperature, as described previously (Mladinic et al., 2013). The adult spinal cord was dissected out from adult pregnant females, anesthetized with the 10.5% chloral hydrate, 0.4 ml/100 g i.m. and subsequently killed by an intracardiac injection (2 ml) of chloral hydrate.

Experimental protocols

The dissected spinal cords were immediately fixed in 4% paraformaldehyde or maintained for preset times in Kreb's solution at room temperature and then fixed. The p38 inhibitor SB203580 or the JNK/c-Jun inhibitor SP600125 (both from Calbiochem/Millipore, Milan, Italy) was added to the Kreb's solution for 12 or 24 h. To induce moderate or severe excitotoxic spinal cord injury, either 50 μM or 1 mM kainate was added to the Kreb's solution for 1 h and then washed out in Kreb's solution for further 24 h (this procedure has previously been described in detail by Taccola et al., 2008; Mladinic et al., 2013). The ischemia-like metabolic perturbation was induced as previously described (Taccola et al., 2008; Bianchetti et al., 2013; Mladinic et al., 2013) by incubating the tissue for 1 h in pathological medium (PM), namely Kreb's solution containing 10 mM H_2O_2, 500 μM sodium nitroprusside, lacking oxygen and glucose, with 6.75–6.80 pH and 230–240 mOsm osmolarity. When the spinal cord was maintained in vitro for 48–72 h, the tissue was kept in oxygenated (95% O_2/5% CO_2) Eagle's basal medium (Sigma-Aldrich, St. Louis, MI, USA) supplemented with 0.2% fetal calf serum, 30 ng/ml 7S nerve growth factor, 10 μg/ml insulin and 0.1 mg/ml gentamycin (Mladinic, 2007).

Fluorescence immunostaining procedure

The free-floating immuno-fluorescence protocol was used as previously described (Taccola et al., 2008; Mladinic et al., 2013). The primary antibodies (Supplemental Table 1) were visualized using appropriate secondary fluorescent Alexa Fluor 488 or 594 antibodies (1:500 dilution, Invitrogen, Carlsbad, CA, USA). Sections were stained in 1 μg/ml solution of 4,6-diamidino-2-phenylindole (DAPI) for 20 min to visualize cell nuclei and mounted on Superfrost Plus (Menzel-Glaser, Braunschweig, Germany) slides. The immunostaining signal was analyzed by Zeiss Axioskop2 microscope (Oberkochen, Germany) or TCS SP2 LEICA confocal microscope (Wetzlar,

Germany), using 1 μm z sectioning. The ATF-3 (C-19, sc-188) antibody (Santa Cruz Biotech, CA, USA) has previously been used as a reliable marker for immunostaining (Tsujino et al., 2000; Tsuzuki et al., 2001; Zhang et al., 2012). The antibody detected the antigen of appropriate sequence since incubation (for 2 h at room temperature prior to immunostaining) with the specific antigenic peptide (Santa Cruz Biotech, sc-188P; dilution 1:5) abolished staining (Supplemental Fig. 1). Quantification of immunofluorescence signals (gray level intensity expressed in arbitrary units, AU) was performed with Meta-Vue imaging software (Molecular Devices, Sunnyvale, CA, USA) using the densitometry function to calculate mean signal intensities for areas of interest (white rectangles) reactive to ATF3 or SOX2 (1000 μm^2 covering the ependymal zone as shown in Fig. 1B for ATF3 and Fig. 4A for SOX2). The values are mean ± SD (at least three different fields in each one of three different sections from two different spinal cords). For each age sample, immunostaining was performed on spinal slices from at least two animals. At least 3 different slices were analyzed for each spinal cord. On each slice, the intensity of the ATF3 or SOX2 immunostaining was measured in at least 3 different fields covering 100 μm^2 large ependymal cell zone around the central canal.

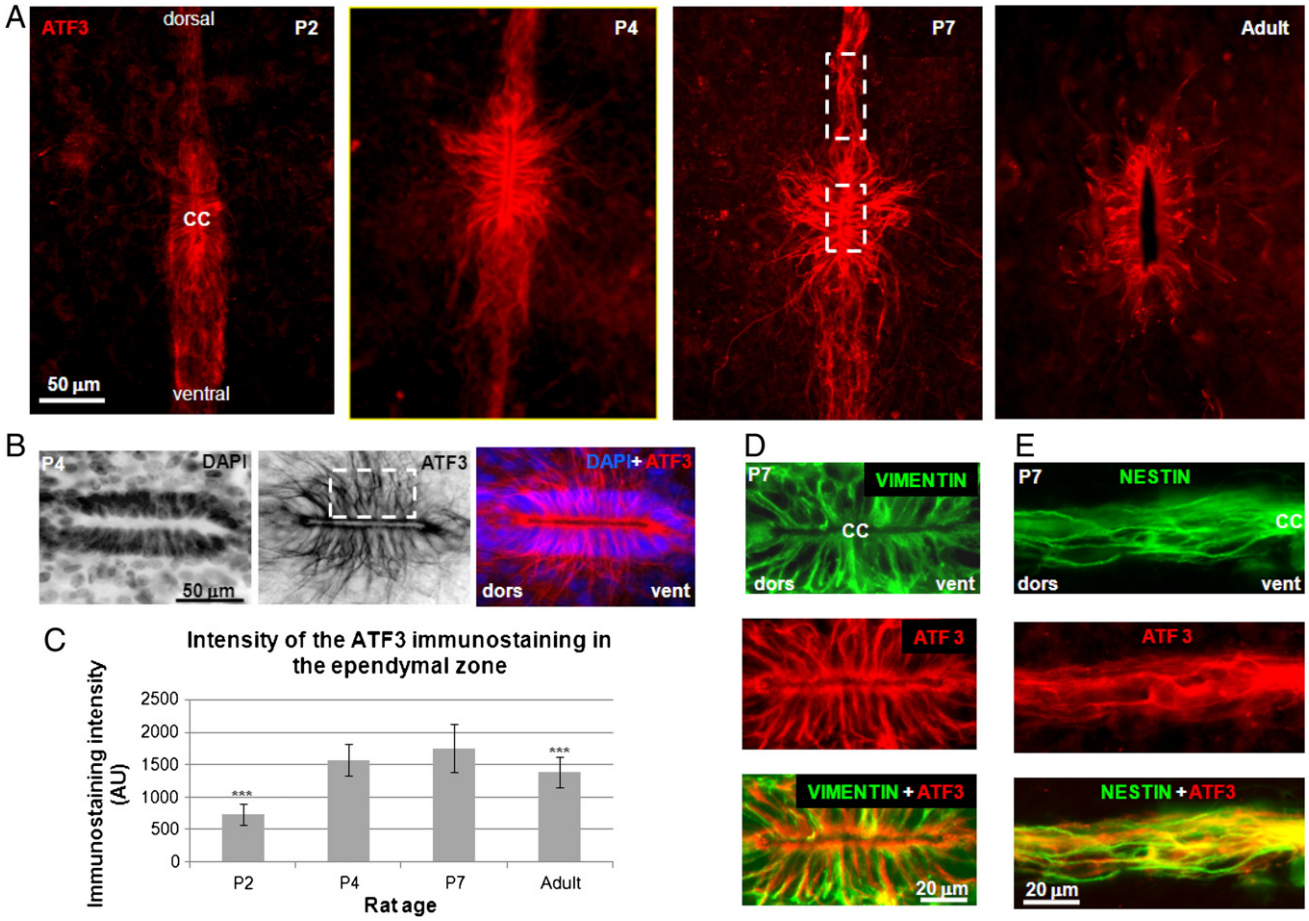

Figure 1 Age-related expression of ATF3 by spinal ependymal cell and its co-expression with nestin and vimentin immunostaining. (A): Examples of cytoplasmic ATF3 immunostaining (red) of the ependymal region around the central canal (CC) of P2, P4, P7 and adult rat spinal cord cross-sections (30 μm thick). (B): Higher magnification of ATF3 immunostaining (with DAPI nuclear counterstaining) of ependymal cells in P4 spinal cord. For image clarity fluorescent stainings (left and middle panels) were converted to grayscale and their negatives are shown to reveal the fibrillary, cytoplasmic ATF3 staining of ependymal cells. In right panel, ATF3 (red) and DAPI (blue) fluorescent stainings are merged. (C): Histograms show the intensity of ATF3 immunostaining (AU) in an area of interest covering the 1000 μm^2 of the ependymal zone (as shown with a white dashed rectangle in B, middle panel) from postnatal day 2, P2, until adult age. The values are mean ± SD (at least three different fields in each one of three different sections from two different spinal cords). The data from P2 and adult spinal cords are significantly different from those obtained from those of P4–7 ($P < 0.001$; One Way Analysis of Variance test). (D): Higher magnification of vimentin immunostaining (green) in the ependymal zone (marked with the lower dashed rectangle in the third panel of A) that overlaps with ATF3 staining (red) as shown by bottom panel in D. (E): Higher magnification of nestin immunostaining (green) in processes extending from ependymal region toward the dorsal funiculus (area marked with the upper dashed rectangle in the third panel of A) that overlaps with ATF3 staining (red) as shown by bottom panel in E. Scale bars = 50 μm (A,B) or 20 μm (D,E). dors = dorsal side of the spinal cord; vent = ventral side of the spinal cord.

Quantification of ATF3, Ki67 or EdU positive cell nuclei

To analyze mobilization of stained cells, ATF3, Ki67 or 5-ethynyl-20-deoxyuridine (EdU) nuclearly labeled cells were counted in a central spinal region (termed funicular migratory stream, FMS; 150 μm wide) that, as shown in Fig. 3C, included a sagittal area from the apex of the dorsal funiculus to the apex of the ventral funiculus. The proliferation assay Click-iT® EdU (Invitrogen) was used in accordance with the manufacturers' instructions as recently detailed (Mazzone et al., 2013). Thus, the spinal cords were incubated for 6, or 24 h in Kreb's solution or for 48 h in Eagle culture medium (see Experimental protocols) containing EdU (10 μM), then fixed, cryopreserved and microtome-sectioned. Incorporated EdU was detected with the fluorescent azide coupling reaction. Sections were then washed twice with 3% BSA in PBS and immunostained with ATF3 or Ki67 antibody.

Western blotting

Cytoplasmic and nuclear fractions were separated by a standard procedure (Kuzhandaivel et al., 2010). Quantification of protein content was performed using a bicinchoninic acid test. Gel electrophoresis was performed on 12% acrylamide SDS gels. As a size standard, Page Ruler Prestained Protein Ladder (Fisher Scientific SAS, Illkirch Cedex, France) from 10 kDa to 170 kDa was used. As positive control, we used RAW 264.7 Cell Lysate (sc-2211, Santa Cruz Biotech). The membrane was incubated with anti-ATF3 (ATF-3, C-19, sc-188, Santa Cruz Biotech) diluted 1:100 in blocking solution. For the negative control, the primary antibody was pre-incubated with the specific blocking peptide (Santa Cruz Biotech, sc-188P; dilution 1:5). Blots were incubated overnight at 4°C. The signal was visualized using fluorescence-labeled secondary anti-rabbit antibodies, produced in goat, with 1:2000 dilution (Dako Italia, Milan, Italy). The results were acquired using Alliance LD2-77WL (Uvitec, Cambridge, UK) and analyzed with Uviband software (Uvitec). ATF3 levels for the cytoplasmic fractions were normalized for β-actin using a β-Actin–Peroxidase antibody (A3854, Sigma-Aldrich), while the nuclear fractions were normalized for TATA binding protein (AB62126, Abcam, Cambridge, UK).

Data analysis

All data are expressed as mean ± SD, except for the Western blotting where the data are mean ± S.E. Statistical analysis was carried out with SigmaStat 3.1 (Systat Software, Chicago, IL, USA). The statistical analysis of the ATF3 immunostaining intensity measurements in spinal cords of various aged rats was performed using One Way Analysis of Variance test, and then, for the pairwise multiple comparison procedures, the Tukey test was used. The number of measurements in each group was >20 (at least two measurements in each of ten different spinal cord sections from three different animals). For the statistical comparison of the ATF3 and SOX2 immunostaining intensity measurements, the *t*-test was used. The number of measurements in each group was 10 (at least three measurements in each of three different spinal cord sections from two different animals). For the statistical analysis of the number of cells with the ATF3, Ki67 or EdU positive nuclei, the *t*-test was also used. The number of sections on which the counting was performed ranged from 6 to 20 for each experimental protocol. For the statistical analysis of the Western blotting ATF3 signal, data were first assessed as parametric with a normality test (Anova Tukey) and then analyzed with the paired and two tailed distribution Student *t*-test. The signals obtained from two different blots were analyzed, and in each experiment, different protein samples, coming from the three different animals, were collected. Thus, the total number of animals for each experimental group was six.

Results

Postnatal ATF3 expression in spinal ependymal cells overlaps with nestin, vimentin and SOX2

Strong ATF3 immunostaining was detected in the cytoplasm of ependymal cells around the spinal central canal of rats aged from postnatal day (P) 2 up to adulthood (Fig. 1A). The ATF3 filamentous staining in the ependymal zone is clearly observed in Fig. 1B. The intensity of the ATF3 immunostaining in the area of interest of ependymal zone (dashed rectangle in Fig. 1B, middle) was found to increase postnatally, and remained elevated in adulthood (Fig. 1C). ATF3 staining overlapped with vimentin (Fig. 1D and Supplemental Fig. 2) and nestin (Fig. 1E and Supplemental Fig. 3), markers expressed by stem cells of the spinal ependymal region (Hugnot and Franzen, 2011). At neonatal age vimentin costained with ATF3 in the ependymal region, while nestin was prevalently localized to processes extending from the ependymal zone toward the spinal funiculi to morphologically bisect the cord transverse plane (Supplemental Figs. 3A–B). In the ependymal region nestin staining was weak (inset to Supplemental Fig. 3A). As previously reported by (Mokrý et al., 2008), in adult rats nestin staining was observed not only in the ependymal region, but also in the blood vessels, while ATF3 staining remained confined to the ependymal zone (Supplemental Fig. 3D). Ependymal cells from embryonic and PO tissue did not show marked ATF3 staining.

Both neonatal and adult ependymal cells were co-stained for ATF3 and the transcription factor SOX2 (Fig. 2A). The results for P4 and P7 age are shown in Supplemental Fig. 4. Fig. 2B shows, at higher magnification, a central section from a stack of z-plane confocal images of adult spinal ependymal cells that confirmed the cytoplasmic ATF3 and nuclear SOX2 stainings of densely packed cells.

Outside the ependymal zone, no significant ATF3 staining was observed in the gray matter as shown by the spinal cord cross section in the reconstructed Fig. 2C. It is noteworthy, however, that, in the lateral and ventral regions of the white matter, cytoplasmic ATF3 staining was detected in sparse cells at early postnatal age (P1–P4) (Fig. 2D). In these white matter cells (showing ramified morphology similar to the NG2/BrdU positive cells; Horner et al., 2000), cytoplasmic ATF3 and NG2 staining coincided with nuclear SOX2 staining (Figs. 2D–E).

ATF3 staining in the ependymal region did not overlap with any of the following cell-specific markers: NeuN

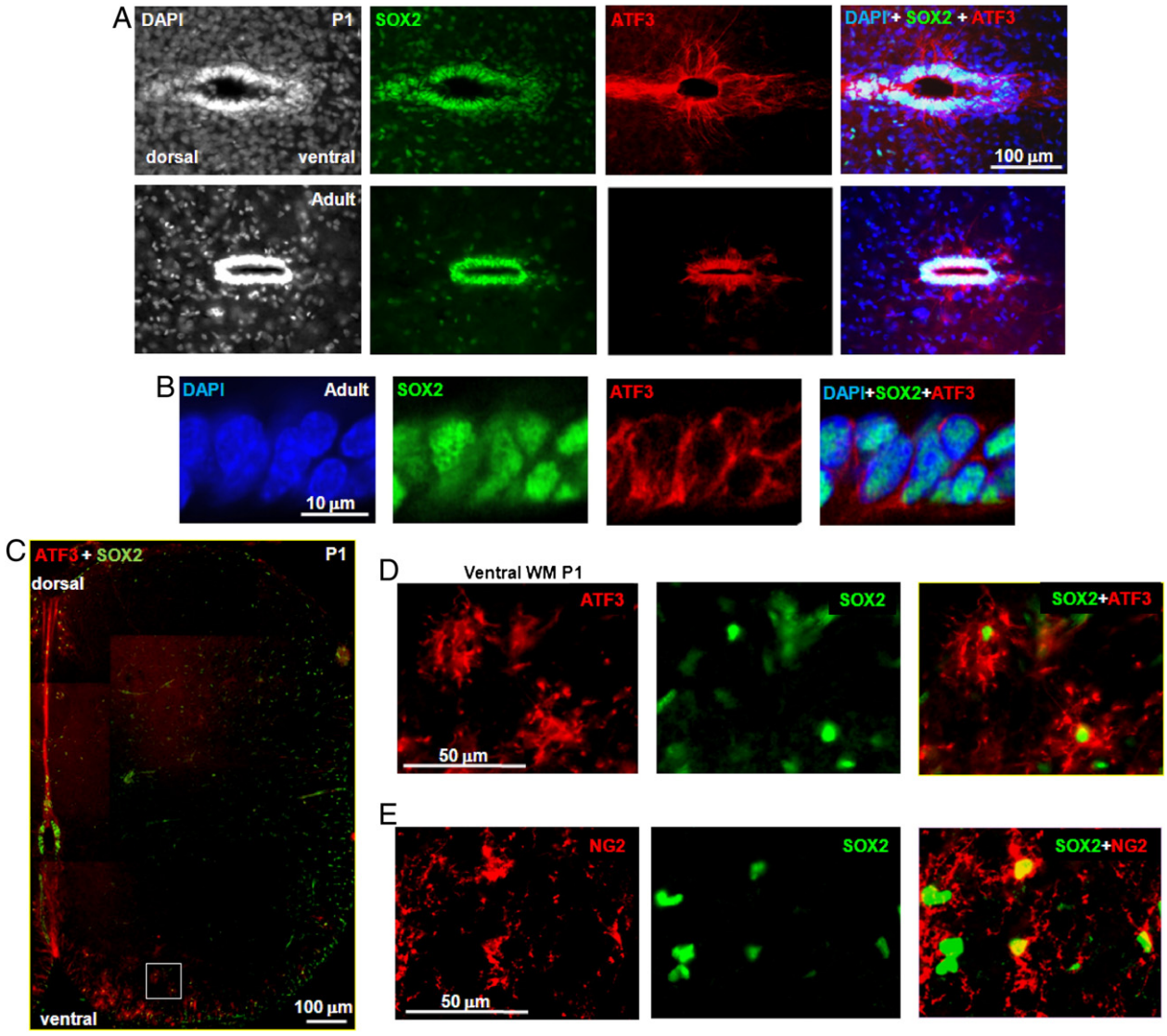

Figure 2 ATF3 immunostaining of ependymal spinal cord cells overlaps with SOX2 in neonatal and adult rats. (A): Spinal cord cross-sections (30 µm thick) of neonatal (top row) or adult (bottom row) spinal cord immunostained with SOX2 and ATF3. The left panels show cell nuclei stained with DAPI (grayscale conversion). In the right panels the fluorescent signals with DAPI (blue), SOX2 (green) and ATF3 (red) are merged. (B): Central section from a stack of z-plane confocal images showing (high magnification) the ependymal zone of adult spinal cord stained with cytoplasmic ATF3 (red), nuclear SOX2 (green) and counterstained with DAPI (blue). (C): Half-section of the P1 spinal cross-section reconstructed from 6 different images (10×). Note that ATF3/SOX2 staining is localized to the ependymal zone, with scattered positive cells in the white matter. (D): Higher magnification of white matter cells with ATF3 cytoplasmic staining (red) and SOX2 nuclear staining (green). (E): Higher magnification of white matter cells with NG2 cytoplasmic staining (red) and SOX2 nuclear staining (green). Scale bar is 100 µm in A,C, 10 µm in D and 50 µm in D,E.

(neurons), DCX (neuronal precursors and immature neurons), GFAP (astrocytes), NG2 (oligodendrocyte precursor cells), O4 (oligodendrocytes and their precursors), or CD68 (activated microglia) (Supplemental Fig. 5). It should be noted that the same ATF3 antibody did not revealed any immunopositive cells in the ependymal spinal cord region of the mouse (results not shown). It has been previously reported that the pattern of ATF3 immunostaining is species-specific (rat or mouse) (Hunt et al., 2012). Furthermore, depending on neuronal type and the intracellular or extracellular milieu, ATF3 may be cytoplasmic and/or nuclear (Seijffers et al., 2006).

In vitro mobilization of ependymal spinal cord cells and nuclear ATF3 expression

Previous studies have indicated that the spinal cord preparation survives in vitro for at least 24 h with functional network activity clearly observed as locomotor-like patterns recorded from multisegmental motor pools (Kuzhandaivel et al., 2011). Fig. 3 shows that such in vitro protocol stimulated mobilization of ependymal cells from the central canal zone toward the dorsal and ventral funiculi (Figs. 3B–D), creating, at 24 h, a characteristic pattern reminiscent of the rostral migratory stream (RMS) of the brain subventricular stem

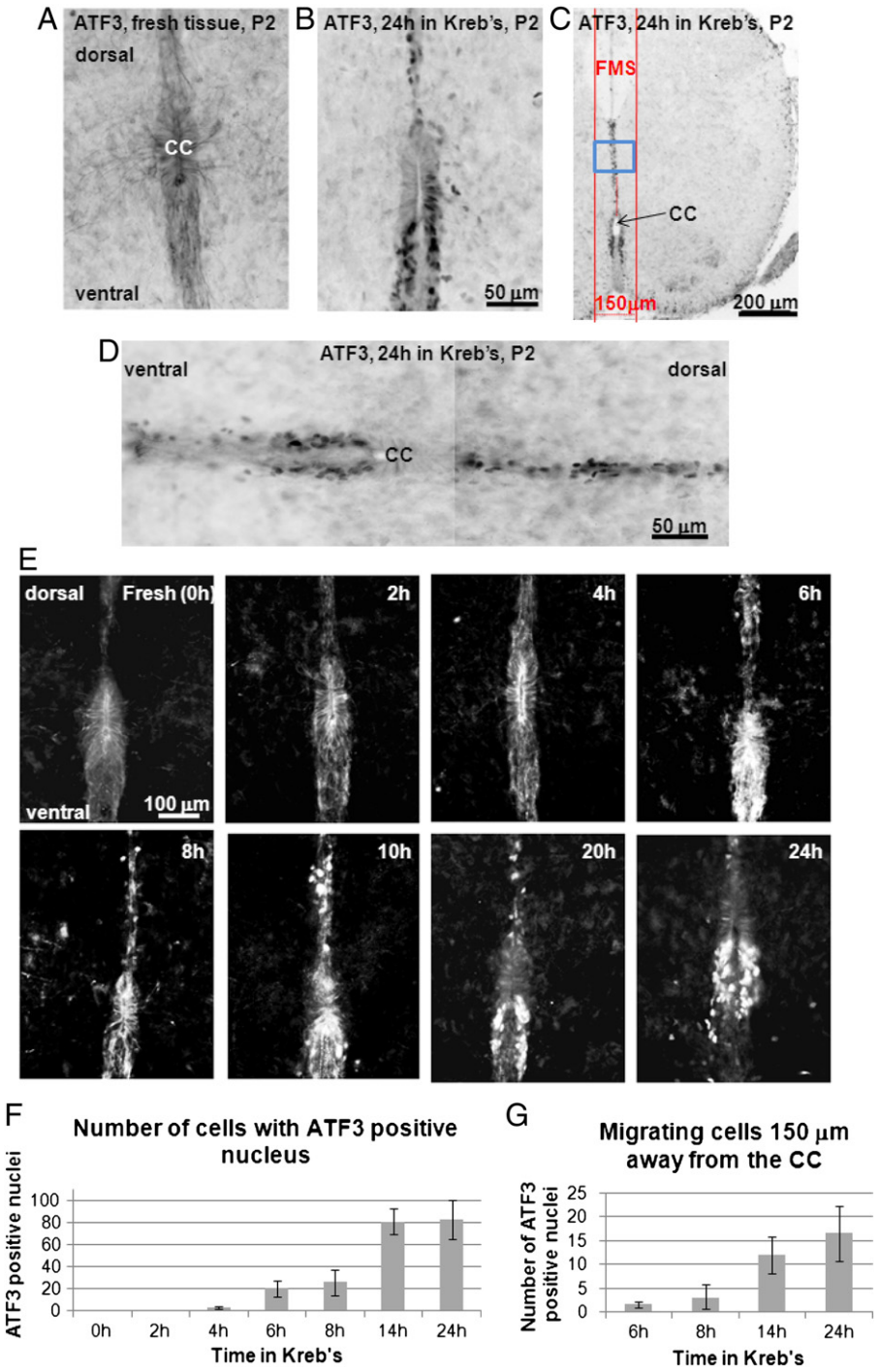

Figure 3 Nuclear ATF3 immunostaining of activated, mobilized stem cells. (A–D): ATF3 immunostaining (grayscale) in 30 μm thick sections from the central zone around the central spinal canal (CC) of P2 rat spinal cord. Note fresh tissue with fibrillar, cytoplasmic ATF3 staining of ependymal cells (A) and nuclear ATF3 staining of cells after 24 h in vitro (B–D) demonstrating migration from the central canal toward the dorsal and ventral spinal funiculi. (C): Half-section of the spinal cord shows the 150 μm wide zone (delimited by red lines) through which the spinal ependymal cells migrate to form the funicular migratory stream (FMS). (D): FMS zone (reconstructed from two images taken at 10×). (E): Grayscale conversion of ATF3 fluorescent immunostaining of P2 rat spinal cords maintained in vitro for 0–24 h, indicating the time course of ependymal cell migration. (F): Number of cells in FMS zone with the nuclear ATF3 staining shows migration started between 4 and 6 h in vitro, and peaked after 24 h. (G): Time-dependent occurrence of ATF3 nuclearly-positive cells in the FMS zone (blue rectangle) 150 μm away from the central canal. Scale bar is 50 μm in A,B and D, 200 μm in C and 100 μm in E.

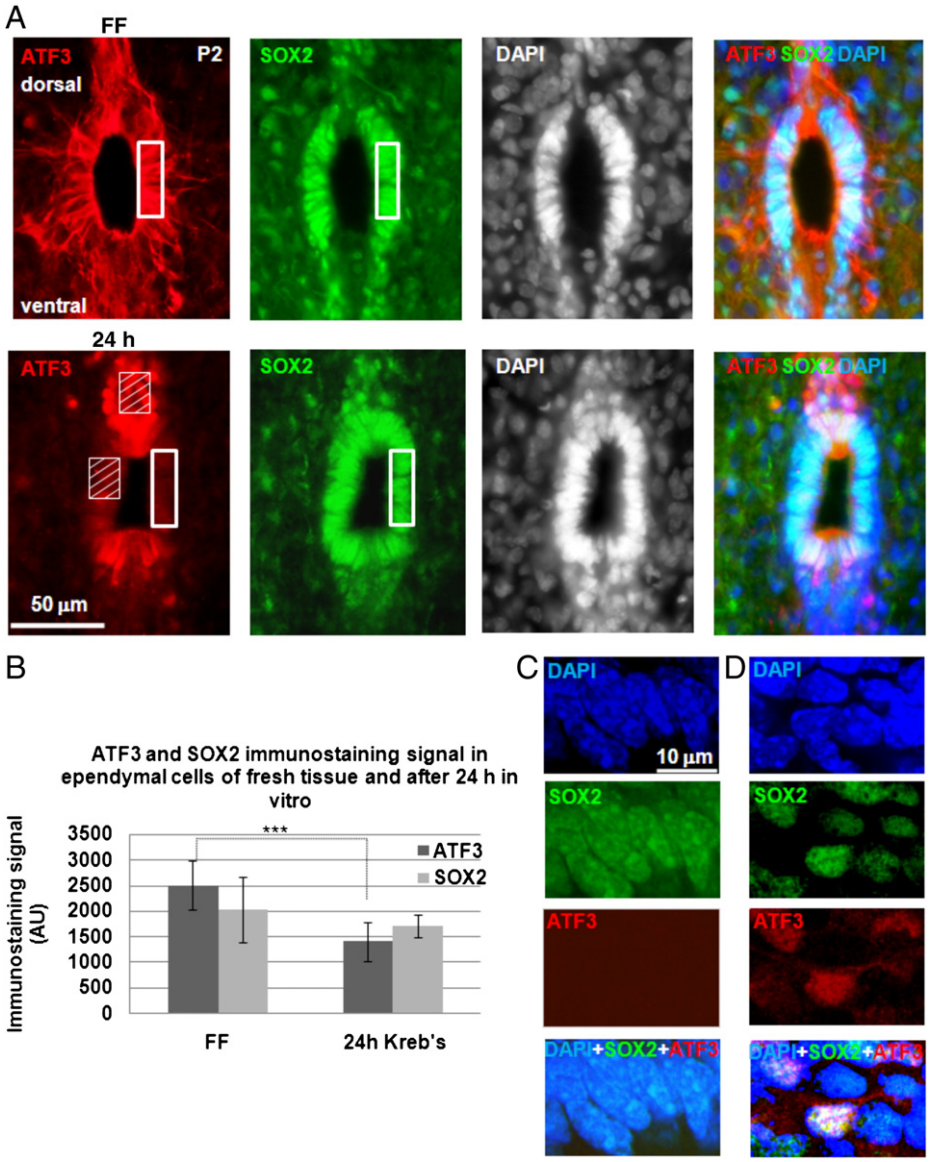

Figure 4 Differential ATF3 and SOX2 immunostaining in ependymal zone of P2 spinal tissue maintained in vitro. (A): Central region of the spinal cord (30 µm thick cross-sections) stained with ATF3 (red) and SOX2 (green) and counterstained with DAPI (grayscale); upper panels show freshly fixed tissue (FF), while lower panels show spinal cord tissue after 24 h in vitro. In right panels the ATF3 (red), SOX2 (green) and DAPI (blue) fluorescent stainings are merged. Note the fibrillary, cytoplasmic ATF3 staining in ependymal cells of fresh tissue, which largely disappears after 24 h in vitro. By contrast, the nuclear SOX staining remains similarly intense in fresh tissue and after 24 h in vitro. (B): Histograms of signal intensity (AU) in the area of interest of the ependymal zone indicated by the white rectangles in (A). Note significant drop of ATF3 signal ($P < 0.001$) after 24 h in vitro while the SOX2 signal did not change. Data are mean ± SD from 10 sections for each group. (C): Confocal images of DAPI (blue), SOX2 (green) and ATF3 (red) staining of ependymal cells of the spinal cord maintained in vitro for 24 h. Bottom hatched box (A, left) indicates the ependymal region used for confocal microscopy. Note the absence of the ATF3 immunostaining signal in (C). (D): DAPI (blue), SOX2 (green) and ATF3 (red) staining of the region apical to the central canal, to which ATF3 nuclearly-positive cells migrate. Note nuclear ATF3 staining overlapping SOX2 nuclear staining. Scale bar = 50 µm in A and 10 µm in C and D.

cells (Coskun and Luskin, 2002; Murase and Horwitz, 2004). By analogy, the spinal cord ependymal migration was termed FMS (see Materials and methods), and was clearly restricted to this 150 µm wide area (Fig. 3C, red lines). The time course of nuclear ATF3 staining is shown in Fig. 3E, and plotted in Fig. 3F. Thus, a detectable ATF3 nuclear signal appeared 4 h after dissection and reached a plateau between 14 and 24 h. Likewise, the occurrence of ATF3 positive cells in the FMS area (indicated by the blue rectangle in Fig. 3C) had a similar time course (Fig. 3G). The ATF3-nuclear positive migratory cells were nestin (Supplemental Fig. 6A), vimentin (Supplemental Fig. 6B) and SOX2 (Supplemental Fig. 6C) positive. Fig. 4A demonstrates the differential distribution of ependymal cell ATF3 staining that was strong around the central canal of fresh tissue (top row in A; region of interest quantified in Fig. 4B), whereas it significantly ($P < 0.001$) decreased (Fig. 4A, bottom

row, and Fig. 4B) at 24 h in vitro. Figs. 4C–D compare the ATF3 expression in two areas of interest (indicated by hatched squares in Fig. 4A, bottom left) and demonstrates that mobilized cells (Fig. 4D) showed nuclear ATF3. On the other hand, nuclear SOX2 staining was consistently found in cells surrounding the central canal in fresh tissue (Fig. 4A, top row) or after 24 h in vitro (Fig. 4A, bottom row) and remained expressed even in the migrated cells (Figs. 4B,D). These results suggest that, while SOX2 was a general stem cell marker, ATF3 preferentially stained nuclei of those ependymal cells undergoing mobilization.

ATF3 is widely used as a marker for axotomized motoneurons (Tsujino et al., 2000), or injured dorsal root ganglion neurons (Tsuzuki et al., 2001). The present study examined ATF3 expression in motoneurons at various times in vitro. ATF3 was detected in the motoneuron cytoplasm already 2 h after dissection, reached a peak at 4 h, after which it decreased with no nuclear staining (Supplemental Fig. 7A). Supplemental Fig. 7B shows, in the same spinal section, strong ATF3 signal in the FMS area (right edge) in contrast with lack of signal from motoneurons (left edge) at 24 h in vitro. At this time point motoneurons were well preserved as shown by their SMI32 staining (Supplemental Fig. 4C) and remain functionally viable (Kuzhandaivel et al., 2011). These results validate ample survival of motoneurons at 24 h in control conditions with no nuclear ATF3 staining characteristic for the injured motoneurons.

To assess if nuclear ATF3-positive migrating cells are able to differentiate into neural cells, we performed double immunostaining of ATF3 and neuron-specific markers such as β-tubulin III and NeuN, or DCX, a neural progenitor marker, in P2 spinal cords maintained in culture for 3 days, to allow abundant migration of ATF3-nuclearly positive cells. Supplemental Fig. 8 demonstrates that ependymal migrating cells remained negative for these markers with rare detection of DCX positivity (arrow in Supplemental Fig. 8).

Proliferative markers of the ependymal region in vitro

The time-dependent redistribution of ATF3 stained cells might have suggested not only mobilization, but also cell proliferation developing during a few hours in vitro. To examine this possibility, we first investigated in the FMS selected region of interest (see Figs. 3C, 5A–C) if cells, which had incorporated EdU as a DNA marker of cell proliferation (Mazzone et al., 2013) also showed ATF3 positivity at 6–48 h in vitro. When the whole FMS region was examined, at 6 h we detected 50 ± 10 EdU positive cells and a lower number of ATF3 nuclear-positive (Edu-negative) cells (20 ± 7; n = 6; Fig. 5D). At 24 h, while the number of EdU positive cells in the FMS area had not changed (52 ± 5; n = 6) vs the value at 6 h (Fig. 5D), the number of ATF3 nuclearly-positive cells increased more than four times (83 ± 18, n = 20). In support of this observation we also studied the number of cells with their nucleus positive for the proliferative marker Ki67 (Mazzone et al., 2013). Fig. 5D shows a similar number of Ki67 or ATF3 positive nuclei at 24 h in the entire FMS region, whereas when the tissue was kept in Eagle culture medium for 48 h, ATF3 staining grew vs Ki67 staining (double immunostaining with Ki67 and ATF3 was not possible for lack of compatible antibodies). Fig. 5C (arrows) also depicts the occurrence of ATF3 and EdU co-staining after 48 h in vitro in the ependymal area. Such ATF3 and EdU double-positive nuclei account for 6.1% ± 1.77 (n = 10) of the total number of ATF3 nuclei in the FMS region. Fig. 5E shows the slow increase in the number of ATF3 and Edu double-positive nuclei over time in culture (6–48 h). Thus, our results suggest that ATF3 nuclearly-stained cells migrated away from the central canal with a time profile distinct from local cell proliferation.

Signaling pathways underlying ATF3 activation

ATF3 activation has been previously shown to be dependent on c-Jun phosphorylation (Lindwall et al., 2004) or the mitogen-activated protein kinases (MAPK)/p38 pathway (Lu et al., 2007). In keeping with this notion, the MAPK-p38 inhibitor SB203580 or the JNK/c-Jun inhibitor SP600125 prevented the rise in the number of ATF3 nuclear-positive cells in the FMS region at 12 h in vitro (Figs. 6A,B). In fact, application of SB203580 (1 μM) or SP600125 (50–100 μM) treatment (12 h) led to absence of nuclear ATF3 signal that was replaced by filament-like, cytoplasmic staining (Fig. 6A).

We next investigated ATF3 protein levels in the nuclear and cytoplasmic extracts from freshly frozen spinal tissue, or maintained for 24 h in Kreb's solution (with or without SB203580 or SP600125). To this end, we used the same anti-ATF3 antibody used for immunostaining previously validated to detect ATF3 protein by Western blotting in cancer tissue (Buganim et al., 2011). The 22 kDa band, corresponding to the full-length ATF3 (Hashimoto et al., 2002; Buganim et al., 2011; Chen et al., 1994), was of the highest intensity in nuclear lysates (loading control was TBP) from spinal tissue maintained in vitro for 24 h (sham; Fig. 6C, top lane, and Fig. 6D), very low from fresh tissue, and significantly ($P > 0.01$) weaker 24 h after SB203580 (1 μM) or SP600125 (100 μM) treatment (Figs. 6C,D). As a positive control, the lysate from RAW 264.7 cells (Abelson murine leukemia virus-induced tumor) was employed, as suggested by the ATF3 antibody manufacturer (see Fig. 6C, right lanes), to produce a strong ATF3 band. Thus, the change in the intensity of the ATF3 specific nuclear expression mirrored the pattern of the ATF3 immunofluorescence signal observed in the nuclei of mobilized cells. Regardless of the protocol used, a band of 28 kDa (as reported by the ATF3 antibody manufacturer) was observed with unchanged intensity in cytoplasmic lysates (β-actin loading control; Fig. 6C, lower lanes).

ATF3 activation after experimental SCI

We recently reported that in vitro spinal cord lesions like excitotoxic injury (Mazzone et al., 2013) or oxygen-glucose deprivation (Bianchetti et al., 2013) applied for a short time (1 h), induce a slowly developing process of cell death that peaks at 24 h. We, therefore, wondered if these paradigms could activate ependymal cell early mobilization. Fig. 7A shows the presence of ATF3 positive cells in the FMS area 24 h after 50 μM kainate application (1 h). Likewise, Fig. 7B depicts, in the same region, ATF3-positive cells 24 h following ischemic-like injury (1 h application of a pathological medium lacking oxygen and glucose and containing reactive oxygen species; Bianchetti et al., 2013). Such cells, with ATF3 positive nuclear staining, were also nestin and

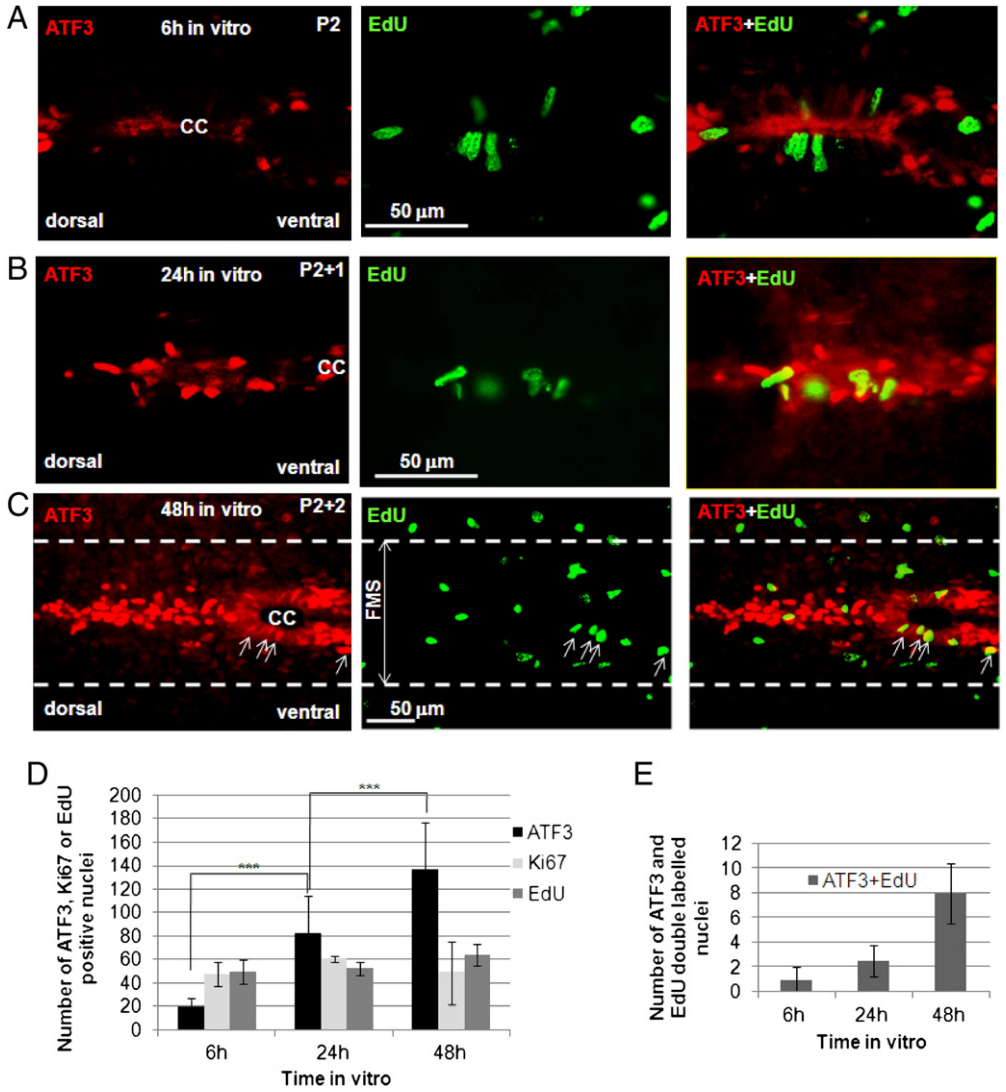

Figure 5 Proliferative cells in funicular migratory stream (FMS). (A,B,C): Nuclear co-immunostaining of ATF3 (red) and EdU (green) in spinal section (30 µm thick) of spinal cord maintained in vitro for 6 h (A), 24 h (B) or 48 h (C). The labeled cells belong to the FMS, the borders of which are denoted by dashed lines in C. Note that the green EdU signal does not overlap with ATF3 positive nucleus in A and B. In C the ATF3/EdU positive cells are marked with arrows. Scale bar = 50 µm. CC = central canal. (D): Histograms showing number of EdU, ATF3 or Ki67 positive nuclei in FMS region of spinal cords maintained in vitro for 6, 24 or 48 h. Note the steady number of proliferative EdU or Ki67 positive cells and significant increase in ATF3 positive nuclei after 24 or 48 h in vitro (***$P \leq 0.001$ for ATF3; n = 6–20 sections from 3 spinal cords). (E): Histogram shows number of ATF3 and Edu double-positive nuclei in FMS region of spinal cords maintained in vitro for 6, 24 or 48 h (n = 3–10 sections from 3 spinal cords).

vimentin positive (Figs. 7A,B). Fig. 7D shows that, with either protocol, the number of cells with the ATF3 positive nucleus in the FMS area was similar to control at 24 h in vitro. Only when the concentration of kainate was raised to 1 mM to apply a very intense excitotoxic stimulus, did the number of ATF3-nuclear positive cells significantly ($P = 0.005$) fall by one-third, suggesting substantial cell loss (Figs. 7C,D).

Discussion

The current study is the first report of the dynamic expression of ATF3 by ependymal spinal stem cells, as this protein was localized to the cytoplasm when such cells were quiescent, but was found in their nucleus when cells became activated. This property enabled us to follow up activated ependymal cells that migrated from the central canal toward the ventral and dorsal white matter, forming the FMS that resembles the RMS of the brain SPCs. The fact that ATF3 immunostaining coincided with well-known SPC markers, such as nestin, vimentin and SOX2, suggests that ATF3 labeling in the spinal cord was primarily expressed by intrinsic stem cells, typically found around the central canal (Hugnot and Franzen, 2011). ATF3 was mainly expressed in the cytoplasm and processes of these cells from P1 onwards, grew during the first postnatal week and remained elevated later. Such ATF3 stained cells in fresh tissue had small diameter, large egg-shaped nucleus, and were closely packed

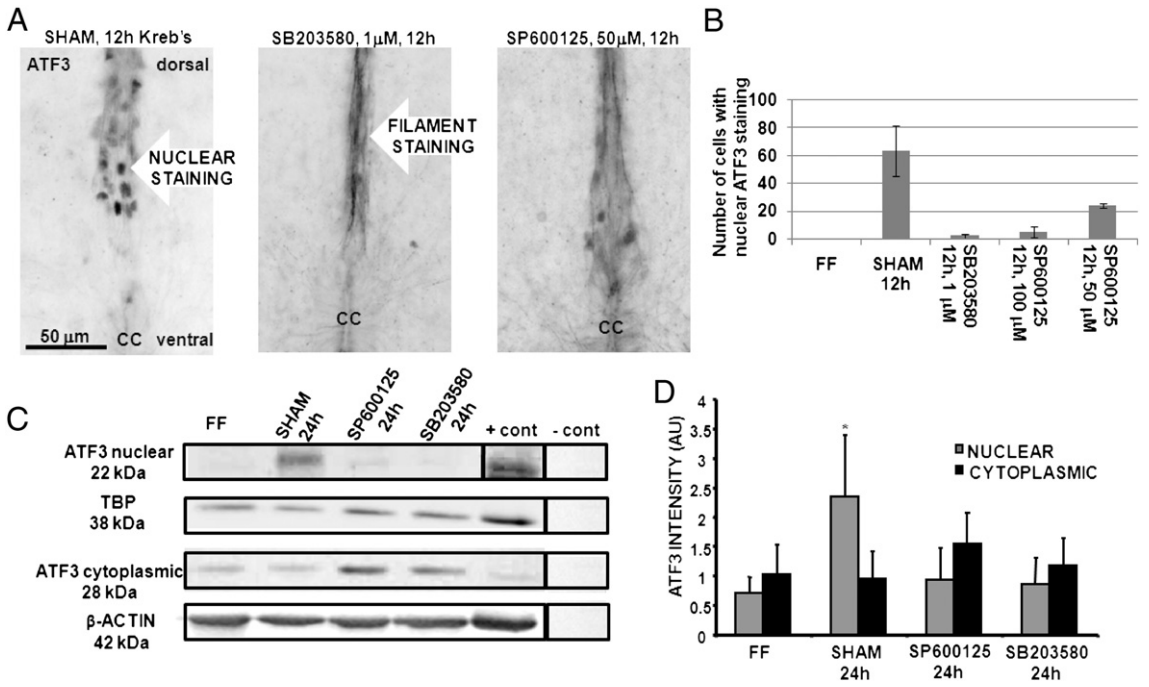

Figure 6 The p38 inhibitor SB203580 or the JNK/c-Jun inhibitor SP600125 blocks nuclear ATF3 staining in spinal cords after 24 h in vitro. (A): Control ATF3 immunostaining (grayscale) in the region near the central canal (CC) after 12 h in Kreb's solution (left, sham; note the intense nuclear ATF3 staining), after treatment with the p38 inhibitor SB203580, or the JNK/c-Jun inhibitor SP600125 for the 12 h. Note filamental ATF3 staining (middle and right panels). Scale bar = 50 μm. (B): Number of cells with nuclear ATF3 staining in the FMS region (delineated with red lines in Fig. 3C) are plotted to show inhibition of cell occurrence after SB203580 or SP600125 treatment (n = 6–20 sections from 3 spinal cords for each condition). (C): Western blots show ATF3 in the nuclear (upper band) and cytoplasmic (lower band) protein fractions from the freshly frozen tissue (FF) or the tissue maintained in vitro for 24 h with or without (SHAM) SB203580 or SP600125 inhibitors. As a positive control, the lysate from RAW 264.7 cells (Abelson murine leukemia virus-induced tumor) is used and the negative control is the result obtained after incubating the ATF3 antibody with the specific blocking peptide prior to immunostaining in the Western blot. The loading control for the cytoplasmic fractions was β-actin and for the nuclear fractions TATA binding protein (TBP). The data were collected from different gels, as indicated by black boxes. (D): Intensity of 22 kDa band ATF3 is of the highest value in nuclear lysates from spinal tissue maintained in vitro for 24 h, when compared to fresh tissue or the tissue treated with the inhibitors ($P > 0.01$; data are duplicate experiments for 6 spinal cords for each condition).

together. Gray matter cells remained, however, devoid of ATF3 staining, adding specificity to the role of this protein for stem cell labeling.

Previous reports of the role of ATF3 in the regulation of SPCs are scant. Recent studies (Gao et al., 2013; Gargiulo et al., 2013) have indicated involvement of ATF3 in the control of genes like SOX2 or BMI1, critical for pluripotency and reprogramming of the human embryonic stem cells or glioblastoma stem-like cells. The present observation of ATF3 and SOX2 co-staining is consistent with this possibility. Moreover, the CREB transcription factor family, of which the ATF3 is a member, has an established role in SPC regulation and neurogenesis (Merz et al., 2011; Mantamadiotis et al., 2012). Our results suggest, however, a new role of ATF3 not only in the maintenance of the spinal ependymal cells but also in their activation.

When spinal cords were kept in vitro for 24 h, we observed a novel phenomenon, namely centrifugal mobilization of ependymal stem cells which formed a migratory chain analogous to the brain RMS (Lois et al., 1996; Wichterle et al., 1997; Tanvig et al., 2009) as they moved away from the central canal to the adjacent ventral and dorsal white matter. When this occurred, ATF3 was clearly expressed in the cell nucleus. This phenomenon developed gradually after 4 h and was fully observed at 24 h. Interestingly, ependymal cells which did not mobilize, retained their SOX2 nuclear staining, yet lost the ATF3 cytoplasmic one. Hence, ATF3 nuclear labeling could be interpreted as a novel marker of migrating ependymal cells. The fact that in vitro conditions induce mobilization of stem cells has been earlier reported with organotypic brain slices (Tanvig et al., 2009): in such a case RMS toward the olfactory bulb is occurring after several days, while the present report shows a much faster process developing within hours. Our proposal of RMS-like migration is currently based on morphological observations only, since these cells did not stain for NCAM, typical marker of RMS in the olfactory bulb (Hu et al., 1996). Thus, we suggest that the unchanged occurrence of Ki67 or EdU positive cells in FMS at 24 h in vitro is compatible with a process of ependymal cell early mobilization rather than proliferation. In support of this hypothesis is the recent observation that, in rat organotypic slices, significant proliferation of neuroprogenitors was detected only after several days in culture (Mazzone et al., 2013). We cannot exclude that ATF3-positive cells might eventually become neurons and/or glia and integrate into spinal networks. This possibility would

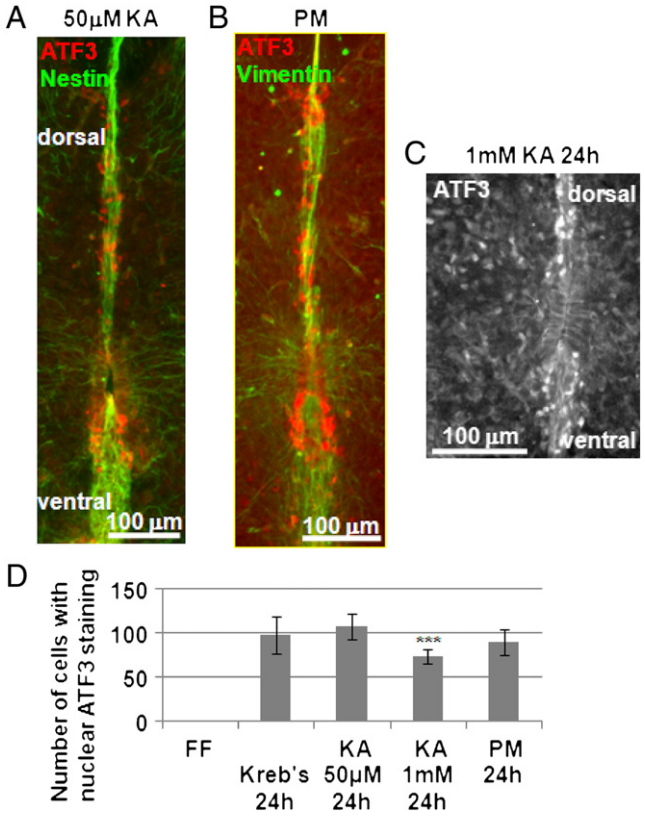

Figure 7 ATF3 positive cells after excitotoxic or ischemia-like spinal injury. (A): ATF3 (red) and nestin (green) double staining of FMS region around the central canal of 30 μm thick sections of spinal cord 24 h after exposure to moderate (1 h long) excitotoxic injury with 50 μM kainate. (B): similar experiment as in A using ATF3 and vimentin co-staining, although the toxic stimulus was 1 h application of pathological medium (PM) mimicking ischemia conditions. (C): very strong excitotoxic stimulus with 1 mM kainate leads to decreased ATF3 signal in the FMS region. (D): The number of the cells with nuclear ATF3 staining in the FMS region (delineated with red lines in Fig. 3C) is significantly ($P = 0.005$) smaller in 1 mM kainate treated spinal cords with 1 mM kainate ($n = 6–20$ sections from at least 3 spinal cords for each group).

assume a delayed maturation process outlasting our observation period limited by tissue survival, and actually absent in spinal slice culture (Mazzone et al., 2013).

The question then arises regarding the mechanism(s) responsible for activation and mobilization of ependymal cells in vitro, given that spinal networks are fully preserved and viable during this timeframe, including electrophysiological activity of locomotor networks (Taccola et al., 2008). In vivo the ependymal cells are in direct contact with the cerebrospinal fluid (CSF) and numerous blood vessels (Hugnot and Franzen, 2011). Thus, their delayed activation in vitro might be due to the disappearance of yet-unclear signals from the CSF or blood (Menezes et al., 2002), which would normally keep the ependymal cells quiescent (Cheung and Rando, 2013). Additionally, the activating signal might come from a few cells injured during dissection, even if systematic analysis of in vitro tissue showed minimal pyknosis at 24 h in vitro (Taccola et al., 2008). A recent review has highlighted how stem cell quiescence is a state maintained by signaling pathways ready to allow rapid activation (Cheung and Rando, 2013). Deciphering the molecular mechanisms regulating stem cell quiescence is, therefore, an important goal for future studies to increase our understanding of tissue regeneration mechanisms in pathological conditions (Cheung and Rando, 2013). Identification of the factors underlying even brain RMS remains incomplete as various chemo-attractants, chemo-repellents, growth factors and cell adhesion molecules have been proposed to guide migrating cells (Menezes et al., 2002; Tanvig et al., 2009). The intracellular presence of other ATF/CREB family members with which ATF3 forms heterodimers may ultimately decide the functional role of ATF3 (Thompson et al., 2009), as much as the influence of regulators like other transcription factors, miRNA or histone modifications (Yun et al., 2010). Future studies are necessary to determine if the FMS pattern of migration detected in vitro appears also in vivo or is due to the experimental tissue preparation with absence of cues from CSF and blood vessels, and if this phenomenon is observed in adult animals as well.

Previous studies have demonstrated that the signal transduction pathways mediating ATF3 expression include c-Jun co-expressed with ATF3 in the nervous system after injury and stress (Hunt et al., 2012). The selective JNK/c-Jun inhibitor SP600125 fully blocks ATF3 induction in adult rat ganglion neurons and inhibits outgrowth of their axons (Lindwall et al., 2004). Furthermore, the MAPK/p38 pathway is also required for ATF3 expression in several non-neuronal cell lines undergoing apoptosis, an effect suppressed by the specific MAPK/p38 inhibitor SB203580 (Lu et al., 2007). In accordance with these results, our current data showed the involvement of both molecular pathways (JNK/c-Jun and MAPK/p38) in the control of the ATF3 nuclear expression in mobilized spinal ependymal cells. This observation was also supported by Western blotting analysis indicating ATF3 expression (of molecular weight in full accord with reports by Chen et al., 1994; Hashimoto et al., 2002) in nuclear fractions at 24 h in vitro. The origin of the variation in the molecular weight between the nuclear and cytoplasmic ATF3 protein remains unclear and will need future work.

Excitotoxic or ischemic-like protocols, that are reported to produce moderate damage to the spinal cord (Taccola et al., 2008; Mazzone et al., 2010; Bianchetti et al., 2013), did not enhance the number of activated and migrating ATF3 positive cells 24 h later. When the excitotoxic stimulus was very strong (1 mM kainate), the number of activated ependymal cells actually decreased in line with widespread neurotoxicity (Taccola et al., 2008). Our previous investigations have indicated that, in the rat spinal cord, neuronal and glial death occurs mainly during the first 24 h (Taccola et al., 2008; Bianchetti et al., 2013; Mazzone et al., 2013). Any attempt to repair cell damage might perhaps require an intervention by stem cells occurring over several days after the primary injury. This process has been examined with long-term organotypic cultures in which stem cell activation two weeks after excitotoxic stimulation failed to produce significant neurogenesis (Mazzone et al., 2013). While ATF3 is reported as a marker for the axotomy-dependent motoneuronal injury in the rat (Zhang et al., 2012), we detected transient, rather early cytoplasmic (never nuclear) staining for ATF3 in motoneurons, a phenomenon that disappeared by 24 h in vitro. Our data, thus, confirm that maintaining the rat spinal cord in vitro did not per se lead to neuron

damage as clearly indicated by fully preserved network responses (Taccola et al., 2008) and that ependymal cell mobilization was probably a reaction to changes in the extracellular milieu.

We propose that the role of ATF3 might be different in the neuronal (postmitotic) and ependymal (mitotic) spinal cells. In neurons ATF3 is viewed as a late marker for injury (Tsujino et al., 2000; Tsuzuki et al., 2001; Francis et al., 2004), with a neuroprotective and pro-survival influence (Zhang et al., 2011; Wang et al., 2012).

Conclusions

In lower vertebrates the spinal cord can regenerate after injury, a process in which ependymal cells play a major role (Hugnot and Franzen, 2011). The mammalian spinal cord, however, cannot regenerate after lesion: hence, intense efforts are in progress to develop new, noninvasive, endogenous-stem cells based strategies for the treatment of spinal injury (Barnabé-Heider and Frisén, 2008; Sahni and Kessler, 2010; Ruff et al., 2012). The discovery of ATF3 as a marker not only for quiescent but particularly for activated, migrating spinal SPCs should help future work to monitor their migration and fate (neurogenesis or gliogenesis) after injury and to test drugs to change the outcome. One might even imagine that it would be possible to up-regulate the ATF3 gene in ependymal spinal cells after injury to find out their impact on the neuronal tissue repair.

Supplementary data to this article can be found online at http://dx.doi.org/10.1016/j.scr.2014.03.006.

Acknowledgments

We thank Mrs Jessica Franzot for technical support with Western blotting. This work was supported by grants from the government of the Friuli Venezia Giulia Region (SPINAL project), the Fund for Transregional Cooperation (MINA project), and the IBRO Return Home Programme Grant (to MM). AD was supported by the project DIANET, 2007/2013 Operational Program of the European Social Fund of the autonomous Region Friuli Venezia Giulia.

References

Barnabé-Heider, F., Frisén, J., 2008. Stem cells for spinal cord repair. Cell Stem Cell 3, 16–24.

Bianchetti, E., Mladinic, M., Nistri, A., 2013. Mechanisms underlying cell death in ischemia-like damage to the rat spinal cord in vitro. Cell Death Dis. 4, e707.

Buganim, Y., Madar, S., Rais, Y., Pomeraniec, L., Harel, E., Solomon, H., Kalo, E., Goldstein, I., Brosh, R., Haimov, O., Avivi, C., Polak-Charcon, S., Goldfinger, N., Barshack, I., Rotter, V., 2011. Transcriptional activity of ATF3 in the stromal compartment of tumors promotes cancer progression. Carcinogenesis 32, 1749–1757.

Chen, B.P., Liang, G., Whelan, J., Hai, T., 1994. ATF3 and ATF3 delta Zip. Transcriptional repression versus activation by alternatively spliced isoforms. J. Biol. Chem. 269, 15819–15826.

Cheung, T.H., Rando, T.A., 2013. Molecular regulation of stem cell quiescence. Nat. Rev. Mol. Cell Biol. 14, 329–340.

Coskun, V., Luskin, M.B., 2002. Intrinsic and extrinsic regulation of the proliferation and differentiation of cells in the rodent rostral migratory stream. J. Neurosci. Res. 69, 795–802.

Francis, J.S., Dragunow, M., During, M.J., 2004. Over expression of ATF-3 protects rat hippocampal neurons from in vivo injection of kainic acid. Brain Res. Mol. Brain Res. 124, 199–203.

Gao, F., Wei, Z., An, W., Wang, K., Lu, W., 2013. The interactomes of POU5F1 and SOX2 enhancers in human embryonic stem cells. Sci. Rep. 3, 1588.

Gargiulo, G., Cesaroni, M., Serresi, M., de Vries, N., Hulsman, D., Bruggeman, S.W., Lancini, C., van Lohuizen, M., 2013. In vivo RNAi screen for BMI1 targets identifies TGF-β/BMP-ER stress pathways as key regulators of neural- and malignant glioma-stem cell homeostasis. Cancer Cell 23, 660–676.

Hashimoto, Y., Zhang, C., Kawauchi, J., Imoto, I., Adachi, M.T., Inazawa, J., Amagasa, T., Hai, T., Kitajima, S., 2002. An alternatively spliced isoform of transcriptional repressor ATF3 and its induction by stress stimuli. Nucleic Acids Res. 30, 2398–2406.

Horner, P.J., Power, A.E., Kempermann, G., Kuhn, H.G., Palmer, T. D., Winkler, J., Thal, L.J., Gage, F.H., 2000. Proliferation and differentiation of progenitor cells throughout the intact adult rat spinal cord. J. Neurosci. 20, 2218–2228.

Hu, H., Tomasiewicz, H., Magnuson, T., Rutishauser, U., 1996. The role of polysialic acid in migration of olfactory bulb interneuron precursors in the subventricular zone. Neuron 16, 735–743.

Hugnot, J.P., Franzen, R., 2011. The spinal cord ependymal region: a stem cell niche in the caudal central nervous system. Front. Biosci. 16, 1044–1059.

Hunt, D., Raivich, G., Anderson, P.N., 2012. Activating transcription factor 3 and the nervous system. Front. Mol. Neurosci. 5, 7.

Kuzhandaivel, A., Nistri, A., Mladinic, M., 2010. Kainate-mediated excitotoxicity induces neuronal death in the rat spinal cord in vitro via a PARP-1 dependent cell death pathway (Parthanatos). Cell. Mol. Neurobiol. 30, 1001–1012.

Kuzhandaivel, A., Nistri, A., Mazzone, G.L., Mladinic, M., 2011. Molecular mechanisms underlying cell death in spinal networks in relation to locomotor activity after acute injury in vitro. Front. Cell. Neurosci. 5, 9.

Lindwall, C., Dahlin, L., Lundborg, G., Kanje, M., 2004. Inhibition of c-Jun phosphorylation reduces axonal outgrowth of adult rat nodose ganglia and dorsal root ganglia sensory neurons. Mol. Cell. Neurosci. 27, 267–279.

Liu, K., Lin, B., Zhao, M., Yang, X., Chen, M., Gao, A., Liu, F., Que, J., Lan, X., 2013. The multiple roles for Sox2 in stem cell maintenance and tumorigenesis. Cell. Signal. 25, 1264–1271.

Lois, C., García-Verdugo, J.M., Alvarez-Buylla, A., 1996. Chain migration of neuronal precursors. Science 271, 978–981.

Lu, D., Chen, J., Hai, T., 2007. The regulation of ATF3 gene expression by mitogen-activated protein kinases. Biochem. J. 401, 559–567.

Mantamadiotis, T., Papalexis, N., Dworkin, S., 2012. CREB signalling in neural stem/progenitor cells: recent developments and the implications for brain tumour biology. Bioessays 34, 293–300.

Mazzone, G.L., Margaryan, G., Kuzhandaivel, A., Nasrabady, S.E., Mladinic, M., Nistri, A., 2010. Kainate-induced delayed onset of excitotoxicity with functional loss unrelated to the extent of neuronal damage in the in vitro spinal cord. Neuroscience 168, 451–462.

Mazzone, G.L., Mladinic, M., Nistri, A., 2013. Excitotoxic cell death induces delayed proliferation of endogenous neuroprogenitor cells in organotypic slice cultures of the rat spinal cord. Cell Death Dis. 4, e902.

McDonough, A., Martínez-Cerdeño, V., 2012. Endogenous proliferation after spinal cord injury in animal models. Stem Cells Int. 2012, 387513.

Meletis, K., Barnabé-Heider, F., Carlén, M., Evergren, E., Tomilin, N., Shupliakov, O., Frisén, J., 2008. Spinal cord injury reveals multilineage differentiation of ependymal cells. PLoS Biol. 6, e182.

Menezes, J.R., Marins, M., Alves, J.A., Froes, M.M., Hedin-Pereira, C., 2002. Cell migration in the postnatal subventricular zone. Braz. J. Med. Biol. Res. 35, 1411–1421.

Merz, K., Herold, S., Lie, D.C., 2011. CREB in adult neurogenesis—master and partner in the development of adult-born neurons? Eur. J. Neurosci. 33, 1078–1086.

Mladinic, M., 2007. Changes in cyclic AMP levels in the developing opossum spinal cord at the time when regeneration stops being possible. Cell. Mol. Neurobiol. 27, 883–888.

Mladinic, M., Nistri, A., Taccola, G., 2013. Acute spinal cord injury in vitro: insight into basic mechanisms. In: Aldskogius, H. (Ed.), Animal Models in Spinal Cord Repair. Neuromethods, 76. Springer Science+Business Media, Humana Press, pp. 39–63.

Mokrý, J., Ehrmann, J., Karbanová, J., Cízková, D., Soukup, T., Suchánek, J., Filip, S., Kolár, Z., 2008. Expression of intermediate filament nestin in blood vessels of neural and non-neural tissues. Acta Med. (Hradec Kralove) 51, 173–179.

Moore, D.L., Goldberg, J.L., 2011. Multiple transcription factor families regulate axon growth and regeneration. Dev. Neurobiol. 71, 1186–1211.

Murase, S., Horwitz, A.F., 2004. Directions in cell migration along the rostral migratory stream: the pathway for migration in the brain. Curr. Top. Dev. Biol. 61, 135–152.

Ruff, C.A., Wilcox, J.T., Fehlings, M.G., 2012. Cell-based transplantation strategies to promote plasticity following spinal cord injury. Exp. Neurol. 235, 78–90.

Sabourin, J.C., Ackema, K.B., Ohayon, D., Guichet, P.O., Perrin, F.E., Garces, A., Ripoll, C., Charité, J., Simonneau, L., Kettenmann, H., Zine, A., Privat, A., Valmier, J., Pattyn, A., Hugnot, J.P., 2009. A mesenchymal-like ZEB1(+) niche harbors dorsal radial glial fibrillary acidic protein-positive stem cells in the spinal cord. Stem Cells 27, 2722–2733.

Sahni, V., Kessler, J.A., 2010. Stem cell therapies for spinal cord injury. Nat. Rev. Neurol. 6, 363–372.

Seijffers, R., Allchorne, A.J., Woolf, C.J., 2006. The transcription factor ATF-3 promotes neurite outgrowth. Mol. Cell. Neurosci. 32, 143–154.

Taccola, G., Margaryan, G., Mladinic, M., Nistri, A., 2008. Kainate and metabolic perturbation mimicking spinal injury differentially contribute to early damage of locomotor networks in the in vitro neonatal rat spinal cord. Neuroscience 155, 538–555.

Tanvig, M., Blaabjerg, M., Andersen, R.K., Villa, A., Rosager, A.M., Poulsen, F.R., Martinez-Serrano, A., Zimmer, J., Meyer, M., 2009. A brain slice culture model for studies of endogenous and exogenous precursor cell migration in the rostral migratory stream. Brain Res. 1295, 1–12.

Thompson, M.R., Xu, D., Williams, B.R., 2009. ATF3 transcription factor and its emerging roles in immunity and cancer. J. Mol. Med. (Berl) 87, 1053–1060.

Tsujino, H., Kondo, E., Fukuoka, T., Dai, Y., Tokunaga, A., Miki, K., Yonenobu, K., Ochi, T., Noguchi, K., 2000. Activating transcription factor 3 (ATF3) induction by axotomy in sensory and motoneurons: a novel neuronal marker of nerve injury. Mol. Cell. Neurosci. 15, 170–182.

Tsuzuki, K., Kondo, E., Fukuoka, T., Yi, D., Tsujino, H., Sakagami, M., Noguchi, K., 2001. Differential regulation of P2X(3) mRNA expression by peripheral nerve injury in intact and injured neurons in the rat sensory ganglia. Pain 91, 351–360.

Wang, A., Arantes, S., Yan, L., Kiguchi, K., McArthur, M.J., Sahin, A., Thames, H.D., Aldaz, C.M., Macleod, M.C., 2008. The transcription factor ATF3 acts as an oncogene in mouse mammary tumorigenesis. BMC Cancer 8, 268.

Wang, L., Deng, S., Lu, Y., Zhang, Y., Yang, L., Guan, Y., Jiang, H., Li, H., 2012. Increased inflammation and brain injury after transient focal cerebral ischemia in activating transcription factor 3 knockout mice. Neuroscience 220, 100–108.

Weiss, S., Dunne, C., Hewson, J., Wohl, C., Wheatley, M., Peterson, A.C., Reynolds, B.A., 1996. Multipotent CNS stem cells are present in the adult mammalian spinal cord and ventricular neuroaxis. J. Neurosci. 16, 7599–7609.

Wichterle, H., Garcia-Verdugo, J.M., Alvarez-Buylla, A., 1997. Direct evidence for homotypic, glia-independent neuronal migration. Neuron 18, 779–791.

Yamamoto, S., Nagao, M., Sugimori, M., Kosako, H., Nakatomi, H., Yamamoto, N., Takebayashi, H., Nabeshima, Y., Kitamura, T., Weinmaster, G., Nakamura, K., Nakafuku, M., 2001a. Transcription factor expression and Notch-dependent regulation of neural progenitors in the adult rat spinal cord. J. Neurosci. 21, 9814–9823.

Yamamoto, S., Yamamoto, N., Kitamura, T., Nakamura, K., Nakafuku, M., 2001b. Proliferation of parenchymal neural progenitors in response to injury in the adult rat spinal cord. Exp. Neurol. 172, 115–127.

Yun, S.J., Byun, K., Bhin, J., Oh, J.H., Nhung le, T.H., Hwang, D., Lee, B., 2010. Transcriptional regulatory networks associated with self-renewal and differentiation of neural stem cells. J. Cell. Physiol. 225, 337–347.

Zhang, S.J., Buchthal, B., Lau, D., Hayer, S., Dick, O., Schwaninger, M., Veltkamp, R., Zou, M., Weiss, U., Bading, H., 2011. A signaling cascade of nuclear calcium-CREB-ATF3 activated by synaptic NMDA receptors defines a gene repression module that protects against extrasynaptic NMDAreceptor-induced neuronal cell death and ischemic brain damage. J. Neurosci. 31, 4978–4990.

Zhang, Z.J., Dong, Y.L., Lu, Y., Cao, S., Zhao, Z.Q., Gao, Y.J., 2012. Chemokine CCL2 and its receptor CCR2 in the medullary dorsal horn are involved in trigeminal neuropathic pain. J. Neuroinflammation 9, 136.